UA9 Results from Crystal Collimation Tests in the SPS & Future Strategy

Scandale, W (CERN)

25 July 2013

The research leading to these results has received funding from the European Commission under the FP7 Research Infrastructures project EuCARD, grant agreement no. 227579.

This work is part of EuCARD Work Package **4: AccNet: Accelerator Science Networks**.

UA9 Results from Crystal Collimation Tests in the SPS & Future Strategy

Scandale, W (CERN)

25 July 2013

The research leading to these results has received funding from the European Commission under the FP7 Research Infrastructures project EuCARD, grant agreement no. 227579.

This work is part of EuCARD Work Package **4: AccNet: Accelerator Science Networks**.

UA9 Results from Crystal Collimation Tests in the SPS & Future Strategy

Introduction

Charged particles entering a crystal at sufficiently small angles with respect to the crystal planes can be captured in channeling states thus performing quasi-harmonic oscillations between the crystal planes. Trajectory confinement is determined by the average electric field of the ordered atoms. Particle channeling is still possible if the crystal is moderately bent up to a critical radius. Particles channeled in a bent crystal are deflected by the bend angle. This provides a powerful method to steer particle beams that has been investigated and already occasionally exploited for some decades.

The UA9 Collaboration supported by CERN, INFN, Imperial College, LAL, PNPI, IHEP and JINR investigates how tiny bent crystals could assist and improve collimation process in modern hadron colliders, such as the LHC, in view of ultra-high luminosity operation. The launch of this collaboration and the preparation of beam experiments were supported by two workshops organized in the frame of EuCARD WP4, i.e. the AccNet-EuroLumi Workshops on Crystal Collimation held at CERN on 9-10 November 2009, and on 25-26 October 2010.

Halo particles surrounding the beam core in a high-intensity high-energy hadron collider in general produce losses in sensitive areas of the accelerator endangering its operation. Multi-stage collimation systems are used to absorb the beam halo. A bent crystal used as a primary collimator instead of a solid target will act as a knife to excise the incoming halo, by deflecting halo particles coherently at large angles and directing them into a secondary collimator-absorber. In this ideal case, a secondary collimator would absorb the beam halo, potentially reducing the losses outside collimation regions.

From 2009 onwards the UA9 Collaboration successfully tested silicon crystals at the SPS providing collimation efficiency measurements with various methods and detectors.

The usage of crystals for collimation purposes at the LHC would pose novel challenges. In steady conditions, a bent crystal could deposit up to 0.5 MW power during several seconds in a small spot on the collimator-absorber that should sustain it without damage. The angular acceptance for channeling is reduced with increasing particle energy. Alignment mechanisms with angular accuracy beyond the state of the art are therefore required and are being developed in partnership with industrial companies. The growth rate of the beam halo is so slow that the first impacts on the crystal occur in a region not exceeding a few atomic layers. This imposes the requirement to have a flat surface parallel to the crystal planes with an unprecedented tolerance. The global requirements for crystal-assisted collimation call for technological breakthroughs in a multidisciplinary range of issues related to beam manipulation, particle detectors, computing and data analysis. UA9 intends to provide solutions for them.

The main findings

The results described below are extracted from Refs [1, 2].

1. Crystal-assisted collimation with protons and Pb-ion beam is extremely successful and the measured collimation efficiency is large. However, the crystal resistance to irradiation with high-energy heavy ion beams should be thoroughly investigated to better estimate the possibility of using a crystal primary collimator for the LHC ion beams. In channeling mode, the loss reduction downstream of the crystal is smaller for Pb-ions, than for protons. Two concurrent effects are responsible for this: during the crystal traversal in non-aligned orientations, ion beams have more nuclear interactions and larger ionization loss resulting in the increase of the oscillation amplitudes. As a result the ion extraction towards the absorber is faster and the potential improvement in channeling is smaller.

2. In channeling condition, the beam loss rate downstream of the crystal is strongly correlated to the off-momentum halo population generated by the collimation process. Both the loss rate downstream of the crystal and the off-momentum population are produced by non-channeled halo fraction. The collimation leakage decreases with increasing channeling efficiency.

3. Preliminary data on the loss maps in some spot positions of the SPS circumference show that the background rate is smaller when the crystal is in channeling orientation with respect to its amorphous orientation.

Strong reduction of the off-momentum halo population [3]

The updated scheme of UA9 is shown in Fig.1.

Halo particles leaking out of the crystal collimation system in the SPS are mostly off-momentum particles generated in the crystal and in the absorber. To detect off-momentum halo one of the inner targets in the high-dispersion (HD) area immediately downstream of the collimation is used. The target is located in the shadow of the secondary collimator absorber (TAL). The target is either the scraper SC, made of a 10 cm long duralumin bar, or the movable Roman pot (RP) having a 3 cm long stainless steel edge 0.1 mm thick. Fig.2-4 shows the dependencies on the angular position of the crystal C4 (2 mm long) for beam losses observed in the crystal (a) and in the HD area target (b). The simulation results for the number of inelastic nuclear interactions in the crystal are also shown (curves 2).

The off-momentum halo population minima are observed at the same angular positions as the beam loss minima in all cases, for protons of 120 GeV/c (Fig.2) and 270 GeV/c (Fig.3) as well as for Pb ions of 270 GeV/c per charge (Fig. 4). A remarkable similarity of the beam loss dependencies recorded downstream of the crystal and in the HD target is observed for Pb ions. Indeed in this case, the loss reduction in the HD area is practically the same as at the crystal. For protons, instead, in both cases (Fig.2 and 3) the reduction in the HD area is smaller than in the crystal. This different behavior could be explained by a larger fraction of particles being scattered back into the circulating beam from the TAL1 in the case of protons.

More specifically, off-momentum particles are created either by ionization energy loss or by diffractive scattering during the traversal of the crystal and/or of the absorber TAL1. Once created the off-momentum particle should ideally survive the traversal of the crystal and of the TAL, and be lost in the HD region, where the TAL2 is used as a detection collimator (associated with a BLM). The off-momentum surviving protons may exceed the fraction of off-momentum surviving Pb-ions, because at the TAL1 they suffer more events of back-scattering into the circulating beam side, which could contribute to the HD loss.

The far off-momentum halo population is the potential source of collimation leakage and inefficiency. In channeling conditions both with Pb ions and with protons its population was reduced by a factor larger than 7. The simultaneous reduction observed for the beam losses at the crystal is a factor about 9 with 270 GeV/c protons and a factor about 7 with Pb-ions.

The agreement of the simulation results with the experimental data is considerably improved by taking into account the miscut angle between the crystal planes and its surface.

Loss map measurements

Using a high-intensity beam made of four trains of 72 bunches spaced 25 ns for a total of $2 \cdot 10^{13}$ protons at 270 GeV/c the intensity of the halo leakage increases by a substantial amount. This allows collecting BLM signals large enough to produce the loss map around the SPS ring. Fig. 5 shows the beam loss reduction R_{bl} that is the ratio of the BLM signals in amorphous and channeling orientations of the crystal, detected by the BLMs with the same gain of 16 in the whole SPS. The beam losses are strongly reduced in all the ring locations where the BLM sensitivity is sufficient for a reliable observation.

Optimization of the crystal collimator parameters

The crystals used up to 2012 in the UA9 experiment are 2 mm long with the bend angle of about 170 μrad and the bend radius R of about 11 m. In the typical UA9 operational conditions, with 270 GeV beams, a shorter crystal 1 mm long, with a bending radius of 5-6 m and a bending angle of about 200 μrad, is expected to be more efficient in channeling orientation, according to simulations and confirmed by the IHEP experience. Two crystals of about 1 mm length installed in a new IHEP goniometer in the SPS could demonstrate this inference. Figure 6 shows the dependence of the beam losses in 1 mm long QuasiMosaic (QM) crystal on its orientation. The observed loss reduction in the aligned crystal is about 18, which is more than two times larger than it is observed with 2 mm long crystals. This result testifies to the quality and predictive power of the model. The same model indicates the optimal length of the crystals to be 4 mm for the LHC.

During high-intensity runs the circulating beam is made of 288 nominal proton bunches distributed in four batches of 72 bunches each, spaced by 25 ns, with a total circulating intensity of a few 10^{13} particles. The bunching time structure is the same as in the nominal LHC filling scheme. In these conditions, for certain position of the goniometer the e-cloud effect is significant, resulting in a large increase of the residual pressure and in a large loss rate close to the goniometer. To check the nature of the phenomenon we wound a solenoid around one of the goniometers and we powered it so as to produce a 50 Gauss longitudinal field during the e-cloud activity period. This procedure suppresses the e-cloud, strongly reducing the loss and the vacuum pressure. In view of this observation, a carbon coating of the LHC goniometer is foreseen for the future in order to fully prevent e-cloud formation under any circumstances.

An industrially produced goniometer is now available for the SPS. The accuracy, sensitivity and reproducibility of the linear and angular positioning measured at the industry premises and in the CERN laboratory is compatible with the LHC specification. Another goniometer based on piezoelectric control of the rotational stage is under construction for the LHC

Conclusions

The UA9 results with protons and Pb ions at 120 GeV/c and 270 GeV/c per charge collected from 2009 to 2012 give a supplementary indication that crystal assisted collimation is well mastered and understood.

1. With a crystal 1 mm long, fully suited to the SPS beam energy, in channeling orientation the loss rate close to the crystal is reduced by a factor close to 20 and the far off-momentum halo population is reduced by factor 7.

2. The miscut angle between the crystal planes and its surface plays an important role. Taking it into account brings the UA9 experimental data in an excellent agreement with simulation results.

3. The beneficial effect of a crystal primary collimator is global. Although the electronics of the SPS beam loss monitors is not fully adequate for the UA9 running conditions, consistent and reliable indications exist of the fact that the loss map around the SPS circumference shows a strong reduction of losses in channeling orientation.

4. The first industrial goniometer compliant with the LHC specification is now available. Tests with beam should supplement as soon as possible the positive results obtained in the laboratory.

All these indications lend confidence that the UA9 beams tests results can readily be extrapolated to the LHC.

Our favorite strategy is to install two crystals in the LHC ring 1, namely one horizontal and one vertical, in order to initially assist protons and Pb-ions collimation during some test runs. The orientation of the crystal with respect to the beam envelope will be controlled using a piezoelectric driven goniometer. To detect the deflected beam an in-vacuum Cherenkov radiator will be used. The long-term challenges will be twofold. The first is to conceive a secondary absorber that could sustain the nominal flux of the extracted halo particles without damage. The second is stage two crystals per plane in order to guarantee the halo extraction even in the presence of small orbit deviations. Development of a simulation code through adding a crystal model description to a particle tracking code such as SIXTRACK is in progress.

References

[1] UA9 status report for 2012.

[2] W. Scandale et al., Phys.Letters B 703 (2011) 547.

[3] W. Scandale et al., Phys.Letters B 714 (2012) 231.

Figure captions

FIG. 1. Layout of the UA9 experiment in the SPS environment. (a) Crystal-collimator area of UA9. (b) High dispersion area of UA9.

FIG. 2. Beam of 120 GeV/c protons. Curves (1) are the dependencies of beam losses observed at the crystal (a) and in the HD area target (b) on the angular position of the crystal C4. Curves (2) are the dependence of the number of inelastic nuclear interactions of protons in the crystal on its orientation angle obtained by a simulation taking into account the crystal miscut.

FIG. 3. Beam of 270 GeV/c protons. The same as in Fig.2.

FIG. 4. Beam of Pb ions with 270 GeV/c per charge. The same as in Fig.2.

FIG. 5.The beam loss map in the SPS shown as the loss ratio between the crystal in amorphous and channeling orientations.

FIG. 6. The reduction factor of beam losses observed in the QM crystal C2 from amorphous to channeling orientation.

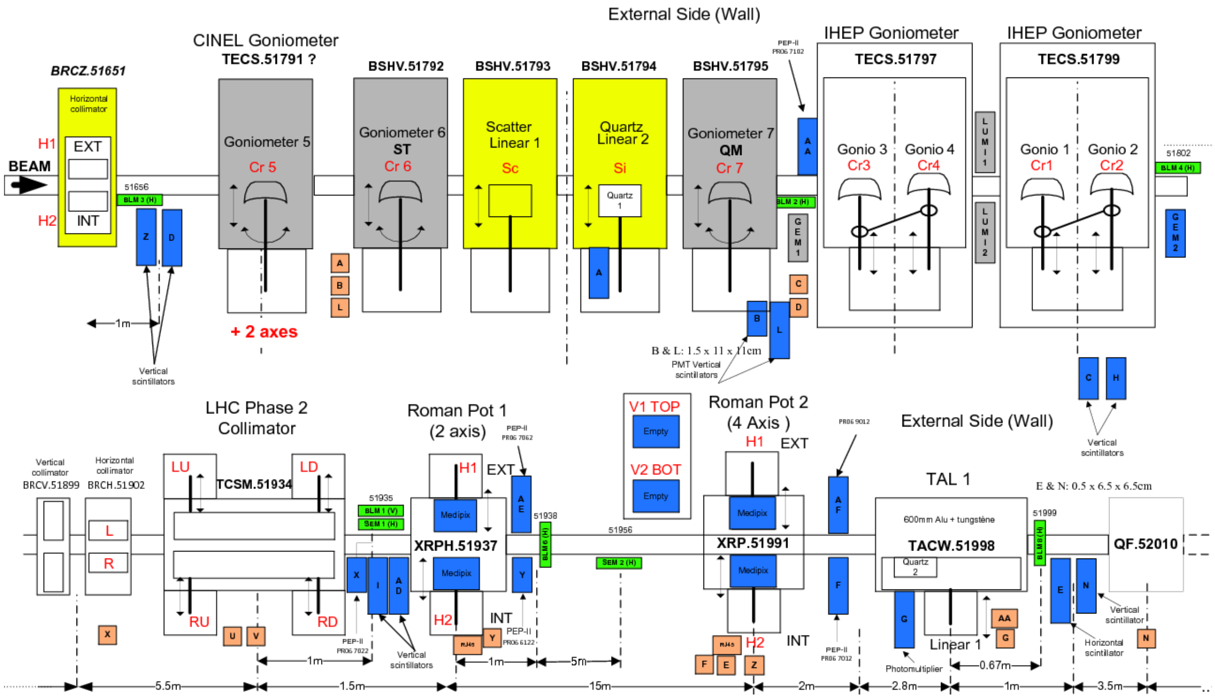

Figure 1a

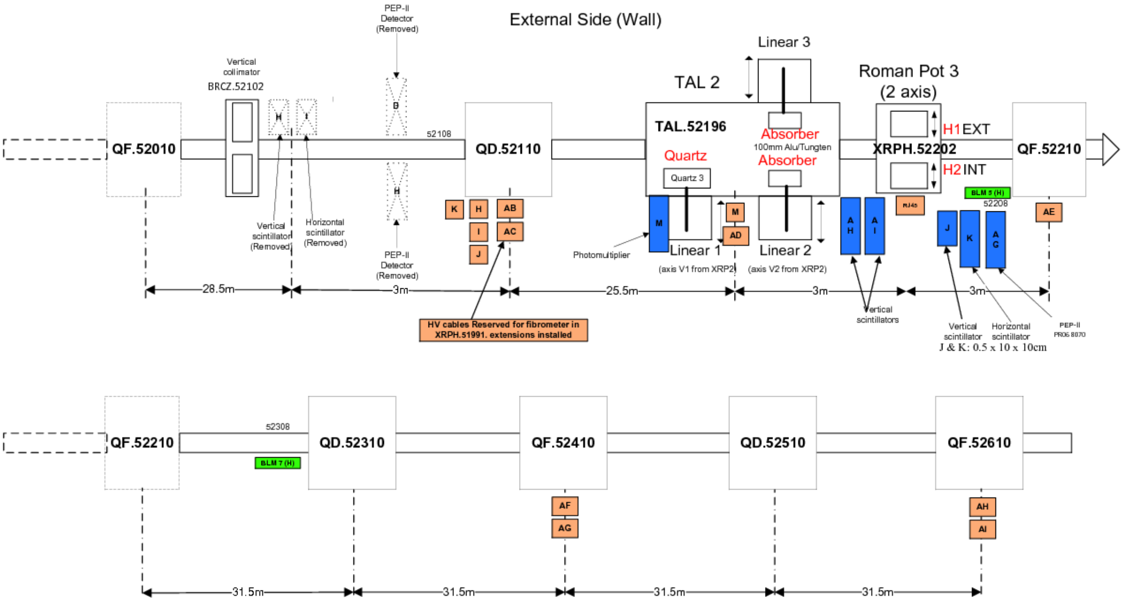

Figure 1b

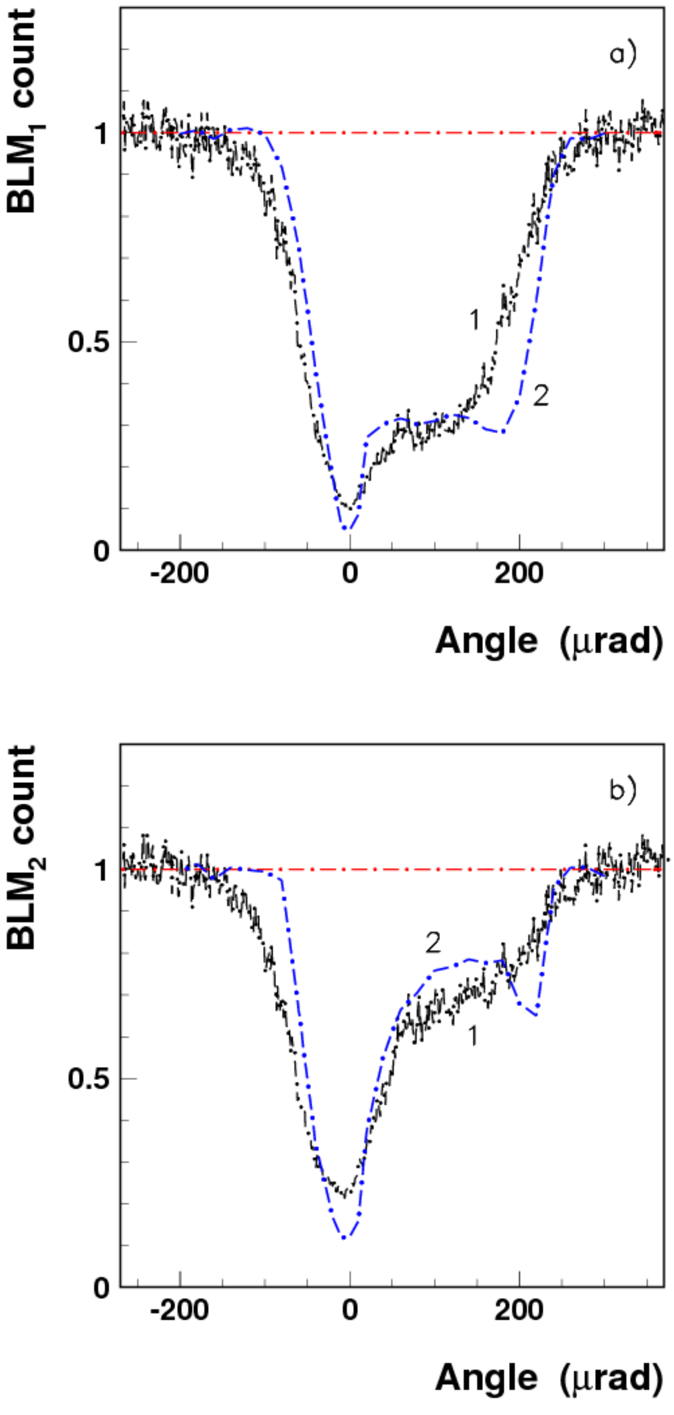
a)
BLM$_1$ count
1
0.5
0
-200
0
200
Angle (μrad)
1
2
b)
BLM$_2$ count
1
0.5
0
-200
0
200
Angle (μrad)
2
1

Figure 2

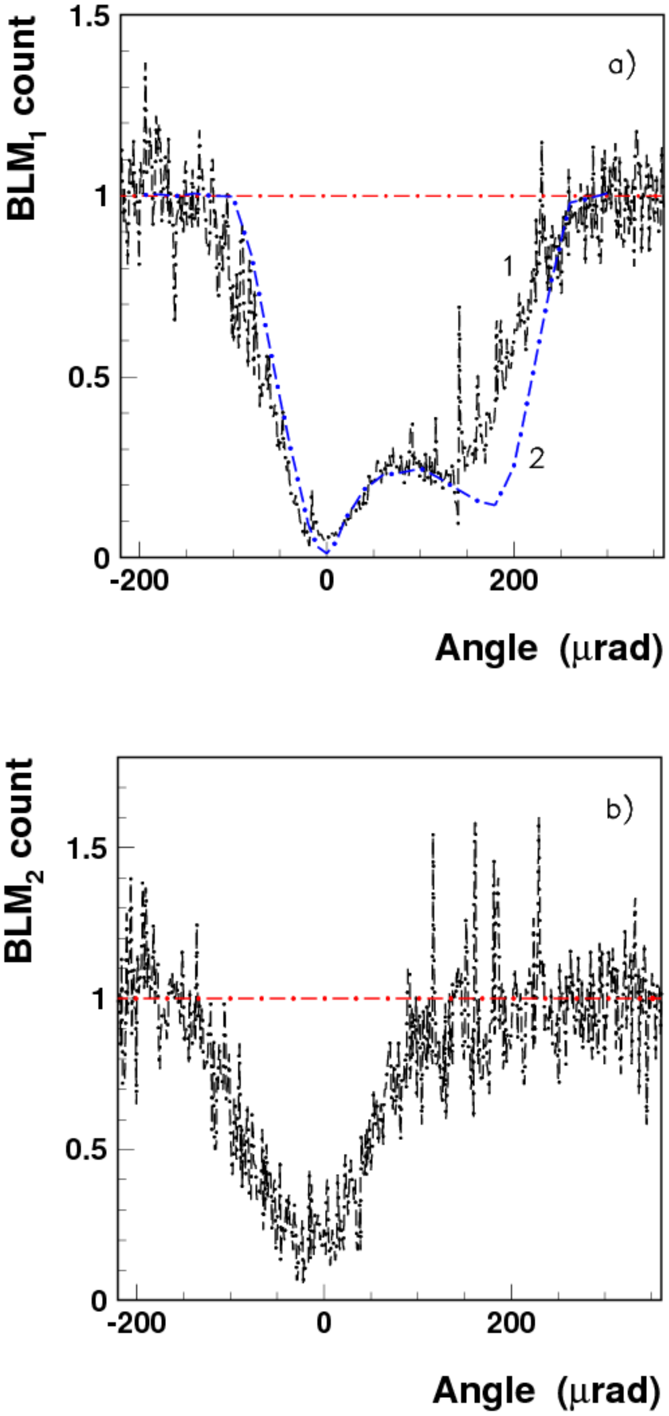
a)
BLM$_1$ count
1.5
1
0.5
0
-200
0
200
Angle (μrad)
1
2
b)
BLM$_2$ count
1.5
1
0.5
0
-200
0
200
Angle (μrad)

Figure 3

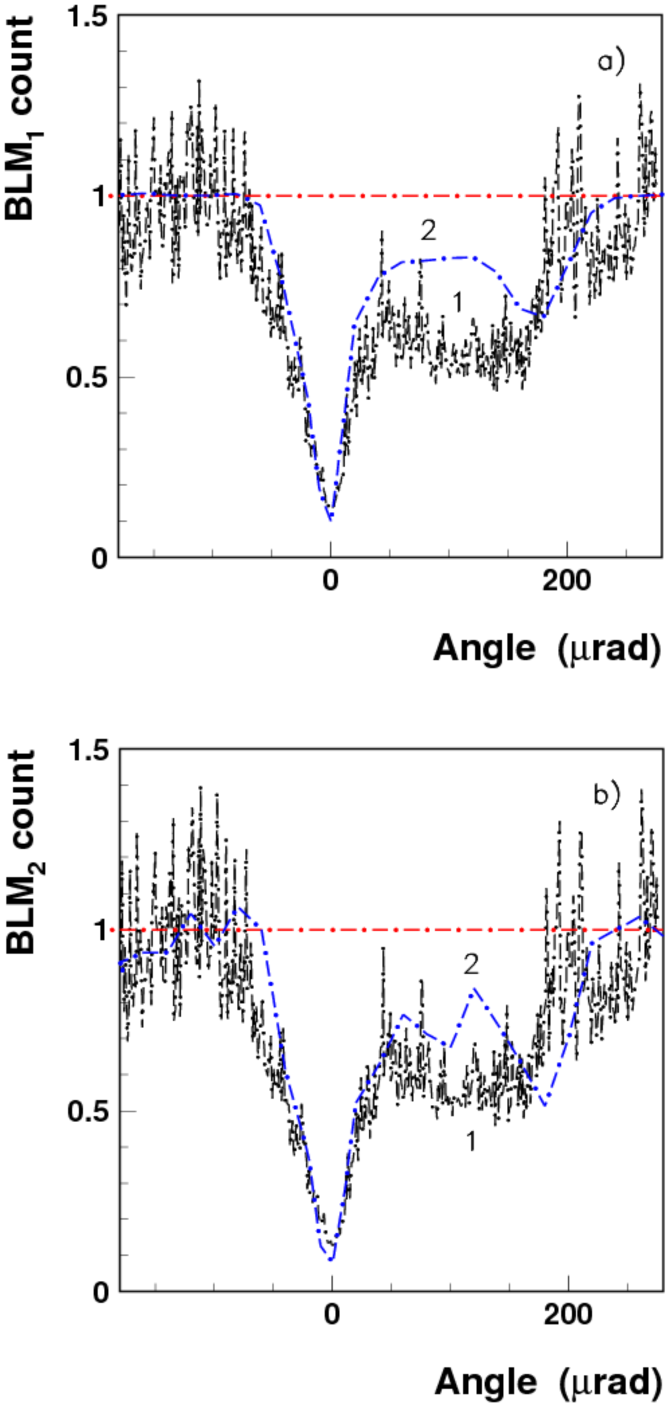
1.5
1
0.5
0
BLM$_1$ count
a)
2
1
0
200
Angle (μrad)
1.5
1
0.5
0
BLM$_2$ count
b)
2
1
0
200
Angle (μrad)

Figure 4

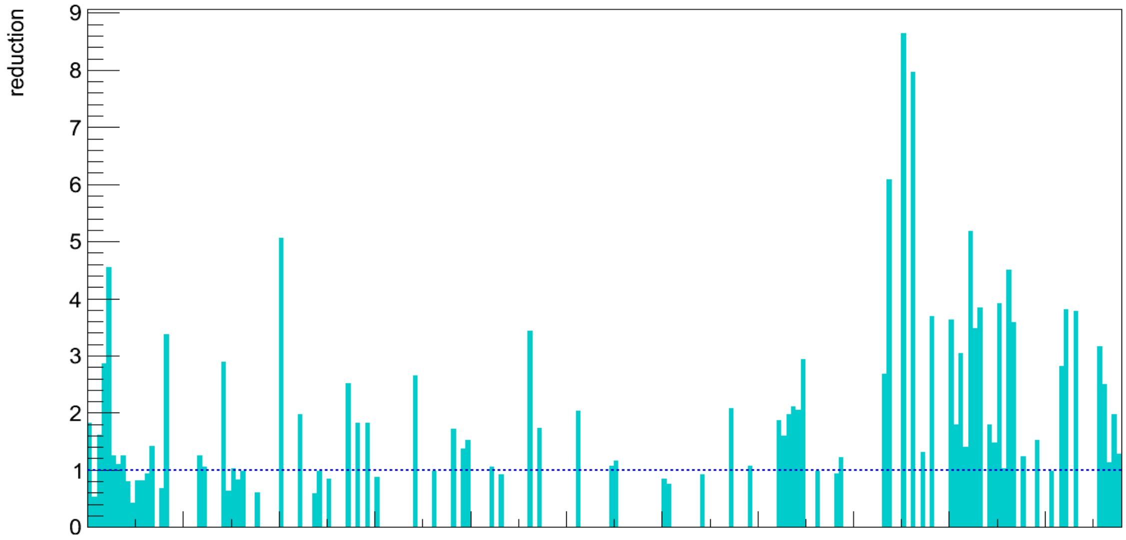

Figure 5

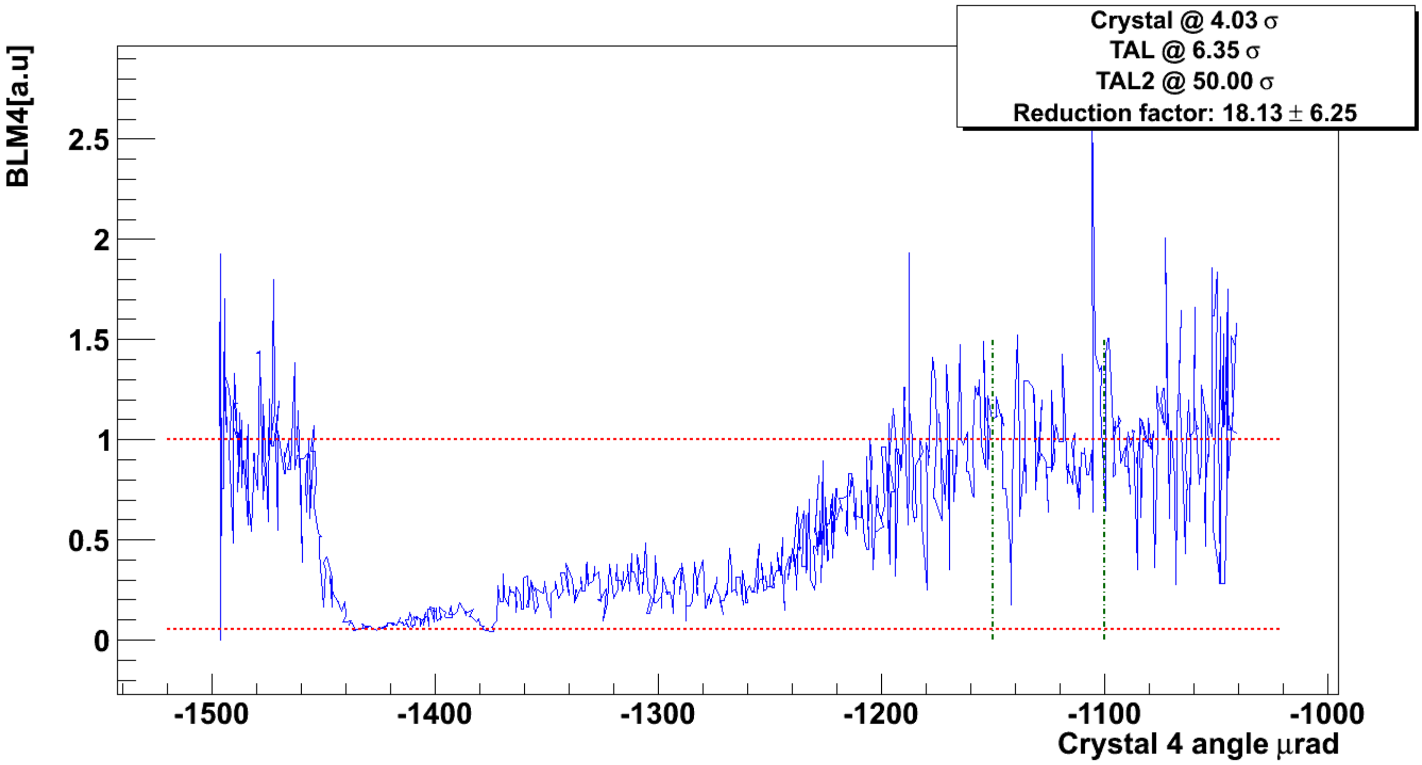
Crystal @ 4.03 σ
TAL @ 6.35 σ
TAL2 @ 50.00 σ
Reduction factor: 18.13 ± 6.25
BLM4[a.u]
2.5
2
1.5
1
0.5
0
-1500
-1400
-1300
-1200
-1100
-1000
Crystal 4 angle μrad

Figure 6